Food and Bioprocess Technology
https://doi.org/10.1007/s11947-022-02763-x

ORIGINAL RESEARCH

Exploring The Potential Acceleration of Granny Smith Apple Drying By Pre-Treatment With CO_2 Laser Microperforation

Eric Araya[1] · Helena Nuñez[1] · Natalia Ramírez[1] · Aldonza Jaques[1] · Ricardo Simpson[1,5] · María Escobar[2] · Pablo Escalona[3] · Oscar Vega-Castro[4] · Cristian Ramírez[1,5]

Received: 9 February 2021 / Accepted: 5 January 2022

Abstract

This study aimed to determine the effect of CO_2 laser microperforation (LMP) pre-treatment in terms of pore density and pore size on the time required for apple (Granny Smith) slices to reach a water activity below 0.4 by means of different dehydration techniques: osmotically dehydration followed by conventional hot air-drying (OD/CD) or refractance window™ technology (OD/RW™) or just drying by means of refractance window™ technology (RW™). Furthermore, a suitable mathematical model for the diffusion phenomenon was implemented. CO_2 laser microperforation was performed on the apple slices in order to reach different pore radius and densities. Apple slices were osmotically dehydrated with a 45°Brix solution at 40 °C before the conventional and refractance window™ treatments, and others were directly dried with a RW™. The drying procedures were performed at 70 °C to reach a water activity (a_w) below of 0.4. The drying time, color change, soluble solid content, and diffusion coefficients (D_{eff}) were determined. Compared to non-microperforated samples, increasing the pores density from 2.86 to 7.94 pores/cm^2 and the pores size from 100 to 300 µm, drying time was reduced in the range of 10 to 60%. The D_{eff} ranged from 5.76×10^{-10} to 11.07×10^{-10} m^2/s for the Fick's second law model and from 0.21×10^{-10} to 5.94×10^{-10} m^2/s$^\alpha$ for the anomalous diffusion model and showed super-diffusive behavior ($\alpha > 1$). Laser pre-treatment favored anomalous diffusion behavior during drying. Collectively, RW™ showed promising results by significantly reducing the control drying time by over 50%.

Keywords Diffusion mechanisms · CO_2 laser · Osmotic dehydration · Refractance window

Introduction

Currently, consumers prefer ready-to-eat food products that provide nutritional properties and contribute to health and overall well-being (Ahmad-Qasem et al., 2015; Landl et al., 2010). Thus, dehydrated foods are a good alternative for developing new food products; however, certain drying methods affect food quality parameters (Hernández et al., 2019). New drying techniques notably improve the nutritional, functional, and visual properties of food (Duarte-Correa et al., 2020; Hernández et al., 2019) to satisfy consumption needs.

Dehydration–reducing the water content of a product–is one of the oldest and most widely used methods for food preservation and considerably reduces chemical and microbial deterioration and facilitates storage and distribution (Lewicki & Jakubczyk, 2004; Sosa et al., 2012). In recent decades, the food industry has used convective drying (CD) to preserve a wide variety of foods at the expense of the

✉ Helena Nuñez
helena.nunez@usm.cl; helenanuneza@gmail.com

1 Departamento de Ingeniería Química Y Ambiental, Universidad Técnica Federico Santa María, P.O. Box 110-V, Valparaíso, Chile

2 Departamento de Química Y Medio Ambiente, Universidad Técnica Federico Santa María, Viña del Mar, Chile

3 Departamento de Industrias, Universidad Técnica Federico Santa María, P.O. Box 110-V, Valparaíso, Chile

4 BIOALI Research Group, Faculty of Pharmaceutical and Food Science, Universidad de Antioquia, Calle 67 No. 53 - 108 Building 2-105, Medellin, Colombia

5 Centro Regional de Estudios en Alimentos Saludables (CREAS) Conicyt-Regional R06I1004, Blanco 1623 Room 1402, Valparaíso, Chile

quality of products sensitive to drying conditions (e.g., temperature, air velocity, and relative humidity) (Fernandes et al., 2015; Sturm et al., 2014). CD modifies the properties of the product, compromises consumer acceptability (Lewicki & Lukaszuk, 2000), and requires significant energy consumption, large storage spaces, and long processing times (Menon et al., 2020). Therefore, new technologies that more quickly and efficiently achieve the same objectives as that of CD at lower industrial costs must be evaluated. Alternatives related to drying process include osmotic dehydration (OD) (Moreno et al., 2013, 2016; Simpson et al., 2015) and refractance window™ drying (Franco et al., 2019; Hernández et al., 2019; Puente-Díaz et al., 2020). On the other hand, technologies that allow to accelerate mass transfer process through structure modifications in food matrices include carbon dioxide (CO_2) laser microperforation (LMP) (Fujimaru et al., 2012; Figueroa et al., 2020; Munzenmayer et al., 2020; Olivares et al., 2021; Ramírez et al., 2021; Veloso et al., 2021), which have been described in recent food-processing studies.

In OD, food is partially dehydrated by immersing it in a hypertonic solution, where water flows from the product to the osmotic solution, and the osmotic solute is transferred from the solution to the product. OD preserves the attributes such as color, firmness, and flavor and increases the shelf life of raw fruits while minimally affecting their quality but is industrially impractical due to the long drying times required to substantially decrease water activity (Corzo & Bracho, 2007; Gallo et al., 2015; Moreno et al., 2013; Simpson et al., 2015; Velickova et al., 2013; Montoya et al., 1999).

Refractance window™ (RW™) drying is a method patented by Magoon (1986) and developed by MCD Technologies, Inc. (Tacoma, WA, USA) that has recently shown potential for drying food, medicine, and cosmetics. RW™ drying is fast, easily scalable, and renders high-quality, energy-efficient products at a lower economic and environmental cost (Menon et al., 2020; Raghavi et al., 2018). The method uses conduction, convection, and radiation heat transfer to dehydrate the product (Mohapatra et al., 2011) in the form of pulp, juice, or thin slices (Clarke, 2004; Raghavi et al., 2018; Sabarez, 2019). The food is placed on a Mylar® sheet placed in a hot water bath; thus, the thermal energy required to evaporate the moisture is transferred from the hot water to the wet material primarily by radiation (Ochoa-Martínez et al., 2012). RW™ technology has recently been used to dry asparagus (Nindo et al., 2003), tomato (Abul-Fadl & Ghanem, 2011), pigmented-flesh potatoes (Kaspar et al., 2012), mango slices (Ochoa-Martínez et al., 2012), chickpea protein isolated extracts (Tontul et al., 2017), mango pulp (Raghavi et al., 2018), salmon, beef, and apple slices (Franco et al., 2019 and Hernández et al., 2019).

LASER, which is light amplified by the emission of stimulated radiation, produces a coherent monochromatic beam with a specific direction to small points, generating destruction with great precision and minimal damage to the surrounding area (Tanzi et al., 2003; Ferraz et al., 2007; Ulloa, 2018). Carbon dioxide (CO_2) lasers are preferred for the treatment of biological matrices, due to their precision, safety, and low environmental impact (Etxeberria et al., 2006; Figueroa et al., 2020). CO_2 laser beam technology is widely used in the medical, cosmetical, and materials industries (Blutinger et al., 2019; Wairimu, 2011). However, this technology has been tested on a few food applications due to its safety, accuracy, versatility, and eco-friendly character (Singh, 2013). The laser produces a specifically targeted monochromatic coherent light beam that focuses on small spot sizes and produces a high-density beam that causes precise tissue destruction and minimal damage to the surrounding area (Tanzi et al., 2003); additionally, the minimal manipulation of the material reduces contamination risks. Several authors (Ulloa, 2018, for lyophilization of a model food; Blutinger et al., 2019, for dough browning; Figueroa et al., 2020, for pork marination and Munzenmayer et al., 2020, for blueberry dehydration; Silva et al., 2020, for tomato peeling) have found that incorporating laser technology improves the quality of the product and reduces the time and energy requirements of the dehydration process.

During food dehydration, diffusion governs the transport mechanisms of solutes and solvents and is commonly modeled by Fick's second law based on an effective diffusivity approach using the solutions proposed by Crank (1975) for different geometries and drying methods. However, various studies show a weak data fit to this model, primarily due to underestimation of the complexity of the problem. Additional phenomena (e.g., heterogeneity in cell structure, shrinkage, volume changes, and protein denaturation) modify the movement of water along the matrix (Corzo & Bracho, 2007; Ochoa-Martínez et al., 2012; Ramírez et al., 2017; Simpson et al., 2015, 2017). An alternative to this problem is anomalous or non-Fickian diffusion, which is based on fractional calculus proposed by Simpson et al. (2013) and considers the changes that occur in the microstructure of the material during the process through an additional parameter in the model (alpha) that improves the fit of the experimental data. This method demonstrates that diffusion is a complex phenomenon involving a series of intervening factors not considered by Fick's second law that explain its significant lack of adjustment (Simpson et al., 2013).

This study aimed to determine the effect of CO_2 laser microperforation (LMP) pre-treatment in terms of pore density and pore size on the time required for apple (Granny Smith) slices to reach a water activity below 0.4 by means of different dehydration techniques: osmotically dehydration followed by conventional hot air-drying (OD/CD) or refractance window™ technology (OD/RW™) or just drying by means of refractance window™ technology (RW™). Furthermore, we aimed to identify a suitable mathematical model for the diffusion phenomenon.

Materials and Methods

Materials

Granny Smith (GS) apples (*Malus domestica*) were purchased from a local supermarket in Valparaíso, Chile and refrigerated at 2.0 ± 0.5 °C until use. Saccharose, potassium sorbate, and calcium chloride ($CaCl_2$) were used for the osmotic solution. An anti-browning solution was prepared using 2% citric acid and 1% ascorbic acid to avoid enzymatic browning of the apple samples after microperforation. All reagents were purchased from G.A. Sales from the city of Viña del Mar, Chile.

Sample and Osmotic Solution Preparation

Apple slices of 0.004 ± 0.0001 m thickness and 0.040 ± 0.001 m diameter (average weight of 0.003 ± 0.00048 kg) were obtained.

An osmotic solution (45°Brix) was prepared for the OD pre-treatment by dissolving 675 g saccharose, 1.27 g $CaCl_2$, and 7 ppm of potassium sorbate in 825 g of distilled water in a 2-L beaker.

Experimental Device

CO_2 Laser Microperforation (LMP)

Different configurations of power, residence time, and number of pulses were tested to obtain three pore sizes (PS) (Table 1) without burning the walls and crossing 100% of the sample. The methodology used by Ramirez et al. (2021) was slightly modified. An optical light microscope (H600 LL HP 100, Hund Wetzlar, Wetzlar, Germany) coupled with a digital camera was used for pore radius measurements. The images containing the pores were analyzed to determine the average pore radius. The pore density (PD, the number of pores per unit area) configuration was conducted in square arrangements of 6 × 6 (2.86 pores/cm^2), 8 × 8 (5.08 pores/cm^2), and 10 × 10 (7.94 pores/cm^2), with equidistant perforations by considering the pore size and the diameter of the sample to be drilled. The LMPs were made to the samples using a SYNRAD TI100 CO_2 laser with a 125-nm lens linked to the computer with WinMarkPro Laser Making Software configuration and adjustment.

Table 1 Different configurations of power, residence time, and number of pulses to obtain the three pore sizes (PS) tested

Parameter	Pore Size (PS)		
	PS1	PS2	PS3
	105 ± 6 μm	198 ± 9 μm	300 ± 11 μm
Power (%) (based on 100 W)	10	25	75
Residence Time (μs)	2	1	1
Number of pulses	120	120	120

Osmotic Dehydration

OD was performed by immersing 136.4 g of the sample in 1.5 kg of osmotic solution maintaining a ratio of 11:1 w/w (solution/samples) according to Simpson et al. (2018). A stainless-steel cylindrical cell was placed in a thermoregulated bath (JEIO TECH, model BS-21) preheated to 40 ± 0.2 °C, with a constant stirring system of 30 rpm. OD was performed until reaching a water activity of 0.95 in the samples.

Convective Drying

The hot air-drying tunnel used for CD consisted of a 1.83-m-long stainless-steel tube with a diameter of 11 cm, an electric fan, and resistance connected to a voltage transformer that adjusts to 120 V (VARIAC SLIDE UP, model SB-10). The air velocity and temperature were set at 2.23 m/s and 70 ± 0.2 °C, respectively, according to the methodology described by Velíc et al. (2004) with slight modifications. The equipment capacity was 16 samples (each sample of 40-mm diameter and 4 mm-thickness) per drying process. The samples were placed on a support in the middle of the tunnel and on an analytical balance of ± 0.001 g (PRECISA, model XB 620 M) configured with Balint Software for continual recording of the weight of the samples at 5-min intervals.

Refractance Window™ (RW™)

A thermoregulated water bath (Mermmet, model WND) was preheated to 70 ± 0.1 °C; the apple samples were placed on the plastic apart from each other, and the frame was placed on an aluminum structure. The Mylar® film was in contact with bubble-free water at the sheet–water interface to form the discontinuous RW™, which consisted of a rectangular metal frame attached to a Mylar® film with thicknesses between 12 and 23 μm. The refractance window™ is highly flexible and moisture and chemical resistant and allows the passage of infrared energy (DUPONT, 2012; Ochoa-Martínez et al., 2012). The Mylar® film dried 18 samples.

In both drying methods, the process ended when the samples reached a water activity (a_w) of 0.4. At $a_w < 0.4$, foods do not show microorganism spoilage (Badui, 2006). In addition, according to Moraga et al. (2011), $a_w < 0.4$ values reduce apple browning. Finally, several authors report that apples present good stability with different drying methods at a_w values < 0.4 (Kahraman et al., 2021; Nieto et al., 2013; Schulze et al., 2014).

The samples used to determine a_w were discarded after the value was obtained. Additionally, we performed a weight control on 3 defined samples at 10-min intervals to calculate water loss over time to evaluate the drying kinetics in each case; these samples were exempt from the a_w determination.

Analytical Determinations

Water activity was determined using a dew-point hygrometer (AQUALAB SERIES 4TE) with a resolution of $\pm 0.0001 a_w$.

The initial moisture content of the samples was determined by drying 5 g of the sample under vacuum conditions in an oven at 60 °C for 24 h and recording the final constant weight (AOAC20013, 1980). The moisture content (M *(g* $_{water}$*/g sample* $_{d.b}$*)*) was calculated using Eq. (1),

$$M = \frac{m_0 - m_d}{m_d} \quad (1)$$

where m_0 (g) is the initial weight of apple and m_d (g) is the dried sample weight after 24 h.

Soluble solids (SS) were determined according to the methodology described by Moreno et al. (2013) using a refractometer (Hanna Instruments, model HI-96801).

The color measurement was performed at the end of drying process, when the samples reached room temperature (20 ± 2 °C) using a colorimeter (Konica Minolta, model CR-410) to measure the coordinates of the CIEL*a*b* uniform color space; L^* was the luminosity, a^* was the red-green hue, and b^* was the yellow-blue hue. The color difference was calculated using Eq. (2), where ΔE indicates the magnitude of the color change between the initial (L_0^*, a_0^* y b_0^*) and final (L_f^*, a_f^* y b_f^*) parameters of the sample to be compared (Sturm et al., 2014). ΔE was obtained for both cases, using a fresh apple and the dried controls for comparison with the dried samples. The ISO12647-2 standard criterion on stability and color ranges was followed to establish significant differences when $\Delta E > 4$ (Pathare et al., 2013).

$$\Delta E = \sqrt{\Delta L^{*2} + \Delta a^{*2} + \Delta b^{*2}} \quad (2)$$

Experimental Design and Statistical Analysis

To analyze the data, a completely randomized design of experiments was performed. The independent variable were the drying treatments, pore density, and pore size. The response variables were the drying time, diffusion coefficients, color change, and soluble solids at the end of the drying process ($a_w < 0.4$).

To establish whether the drying method, pore size, and PD affected the response variables, an ANOVA model was performed with a significance level of 95% (Statgraphics Centurion XV version 16.1.15). To establish whether there were significant differences between treatments, the LSD-Fisher multiple range test was performed ($\alpha = 0.05$). The tests were performed in duplicate.

The experiment was designed using the Statgraphics Centurion XV Software version 16.1.15 (Table 2) following a Box–Behnken design (BBD) to determine the effects of the factors and their interactions on the response variables. We avoided unsuccessful results (extreme points), assessed the interactions, and reduced the total number of experiments to 15, of which 3 corresponded to the central points of the study and were used to assess its significance (Gutiérrez & De la Vara, 2008; Jaramillo et al., 2013).

For all the evaluated drying methods (OD/CD, OD/RW™, and RW™), additional dryings were performed without laser microperforations to evaluate the effect of aforementioned technology on drying. The OD/CD experiment without laser microperforations was considered the control

Table 2 Box–Behnken design for surface analysis with 15 treatments in total, including 3 central points

Treatment	Method	Pore Density (pores/cm^2)	Pore Size (μm)
1	–1	0	–1
2	0	1	1
3	–1	1	0
4	0	1	–1
5	1	0	–1
6	0	–1	1
7	1	–1	0
8	0	0	0
9	1	1	0
10	–1	–1	0
11	1	0	1
12	0	–1	–1
13	0	0	0
14	–1	0	1
15	0	0	0
Factors	**Levels**		
	–1	0	+1
Method	OD/CD	OD/RW™	RW™
Pore Density (pores/cm^2)	2.86	5.08	7.94
Pore Size (μm)	100	200	300

The laser microperforations were performed as a pre-treatment for the 3 drying methods

OD Osmotic dehydration, *CD* Conventional drying, *RW*™ Refractance window™

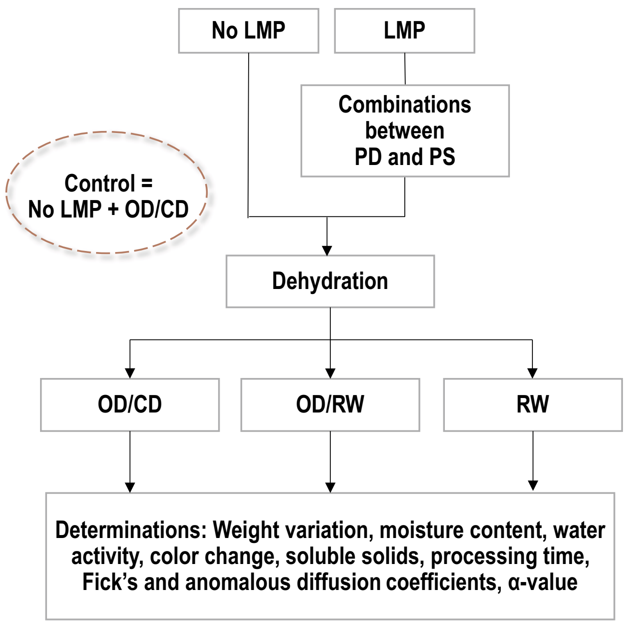

Fig. 1 Experimental design applied for the study of the effect of laser microperforation (LMP) varying pore density (PD) and pore size (PS) on dehydration of apple slices under osmotic dehydration/convective drying (OD/CD), osmotic dehydration/refractance window (OD/RW) and refractance window (RW™)

for the drying process. Figure 1 presents the proposed experimental design.

Mathematical Models

Fick's Second Law of Diffusion

Apple slices correspond to an infinite sheet geometry with unidirectional diffusion, where an isothermal process (70 °C), no sample deformation, and an effective diffusion coefficient (D_{eff}) constant were the assumptions considered in the mathematical modeling (Fig. 2).

The boundary conditions of the system are presented below:

$$M(x,t) = M_0, 0 \leq x \leq L, t = 0 \tag{3a}$$

$$M(x,t) = M_t, 0 \leq x < L, t > 0 \tag{3b}$$

$$M(x = L, t) = M_e, t > 0 \tag{4}$$

Therefore, the dimensionless average water concentration profile can be determined using the analytical solution of Crank (1975) for an infinite sheet, as shown in Eq. (5):

$$MR = \frac{M_t - M_e}{M_0 - M_e} = \frac{8}{\pi^2} \sum_{n=0}^{\infty} \frac{1}{(2n+1)^2} \exp\left(-Deff\left(\frac{(2n+1)\pi}{2L}\right)^2 t\right) \tag{5}$$

where MR is the dimensionless moisture content (moisture ratio), M_t is the water content at t (g water/g sample $_{d.b}$), M_e is the water content at equilibrium and considered as zero (g water/ g sample $_{d.b}$), M_0 is the initial water content at $t = 0$ *min* (g water/g sample $_{d.b}$), D_{eff} is the effective diffusion coefficient (m^2/s), and L is the half-thickness of the sample (m).

Anomalous Diffusion Model

The anomalous diffusion equation based on fractional calculus was proposed by Simpson et al. (2013) and is shown here as a general expression:

$$\frac{\partial^\alpha M}{\partial t^\alpha} = D^*_{eff} \frac{\partial^\beta M}{\partial x^\beta} \tag{6}$$

Fig. 2 Schematic representation of mass and energy flows involved in microperforated apple slice drying using RW™

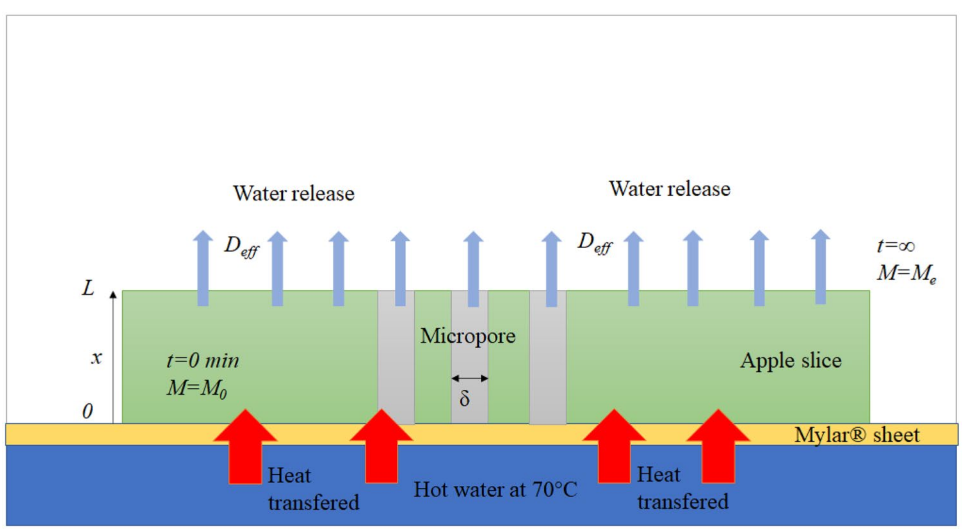

Previous studies (Ramírez et al., 2017; Simpson et al., 2013, 2015) show that fractional and second orders can be used for the temporal (α) and spatial derivatives ($\beta = 2$), respectively, to represent the evolution of mass transport in porous media. Equation (7) corresponds to the anomalous diffusion solution for plane sheet geometry:

$$MR = \frac{M_t - M_e}{M_0 - M_e} = \frac{8}{\pi^2} \sum_{n=0}^{\infty} \frac{1}{(2n+1)^2} E_\alpha \left(-D_{eff}^{*} \left(\frac{(2n+1)\pi}{2L} \right)^2 t^\alpha \right) \tag{7}$$

where E_α corresponds to the Mittag–Leffler function, which is commonly used to solve equations with derivatives of fractional order and reduces to the exponential function when $\alpha = 1$. The α parameter is dimensionless, and D_{eff}^{*} is the effective anomalous diffusion coefficient (m^2/s^α).

An adjustment was made using MATLAB R2019b Software, with programming for n terms of the sum (n = 150). The developed code allowed us to obtain the values of the effective diffusion coefficients (D_{eff} and D_{eff}^{*}), the sum of squared errors (SSE), the coefficient of determination (R^2), and the parameter alpha (α) of the anomalous model.

Results and Discussion

The BBD results were analyzed using one-way ANOVA, which decomposes the contribution of each variable (factors) and their interactions on the response variables (i.e., Fickian and anomalous diffusivities, the alpha parameter, the color change, and the final soluble solids) (Gilpavas et al., 2016a, 2016b).

Table 3 presents the *p-values* obtained from the analysis. The obtained correlation coefficients are not very high; however, the lack of fit yielded *p-values* greater than 0.05, indicating that the measured data fit the model of the design of experiments; that is, the data obtained from drying are represented by a quadratic model (Duarte-Correa et al., 2020).

Figure 3 presents the Pareto charts obtained from the analysis that were used to verify the statistical significance of each factor on each response variable. The parameters of the anomalous diffusion model were significantly influenced by the three principal effects of the studied factors and by the quadratic effect of the drying method (Fig. 3b, c). The anomalous diffusion coefficient is higher for higher pore densities, and the D_{eff}* value ($p < 0.05$) is lower for larger PS. PD had a significantly influence on Fick's diffusion coefficient ($p < 0.05$), which was larger for higher pore densities. The quality parameters are primarily affected by the drying method and its quadratic effect and to the pore size. Changes in color and the content of soluble solids in the samples are greater for larger PS. Thus, the evaluated factors significantly influence process efficiency.

Drying Time Reduction

Table 4 presents the total and per-stage drying times for each experiment (up to $a_w < 0.4$); the data are separated into groups according to the drying method and considering the experiments without laser microperforations. All microperforation treatments decreased the drying time in the OD and the drying stage, either by CD or RW™; this result is interesting, because authors (e.g., Heras-Ramírez et al., 2012) mention a significant effect on the preservation of bioactive compounds and apple quality with reduced drying time. The samples dried only with the RW™ presented the shortest average drying times (between 80 min and 102.5 min), compared to 168.8 –197.5 min for OD/CD. OD pre-treatment significantly increased the drying times; OD alone required from 75 to 95 min to attain a a_w of 0.95.

Table 3 Analysis of variance (ANOVA) of the Box–Behnken design

	P-value				
	Fick Diffusivity	**Anomalous Diffusivity**	**Alpha**	**Color Change**	**Soluble Solids**
A: Method	0.429	0.015	0	0.007	0
B: Pore Density	0.034	0	0.001	0.77	0.089
C: Pore Size	0.388	0.021	0.002	0.037	0.015
AA	0.111	0.001	0	0	0
AB	0.734	0.41	0.298	0.028	0.004
AC	0.843	0.785	0.349	0.427	0.87
BB	0.143	0.046	0.056	0	0.568
BC	0.741	0.136	0.953	0.372	0.011
CC	0.192	0.162	0.797	0.097	0.782
R^2	45.238	77.174	84.527	76.737	91.897
Lack of fit	1	0.306	0.506	0.119	0.988

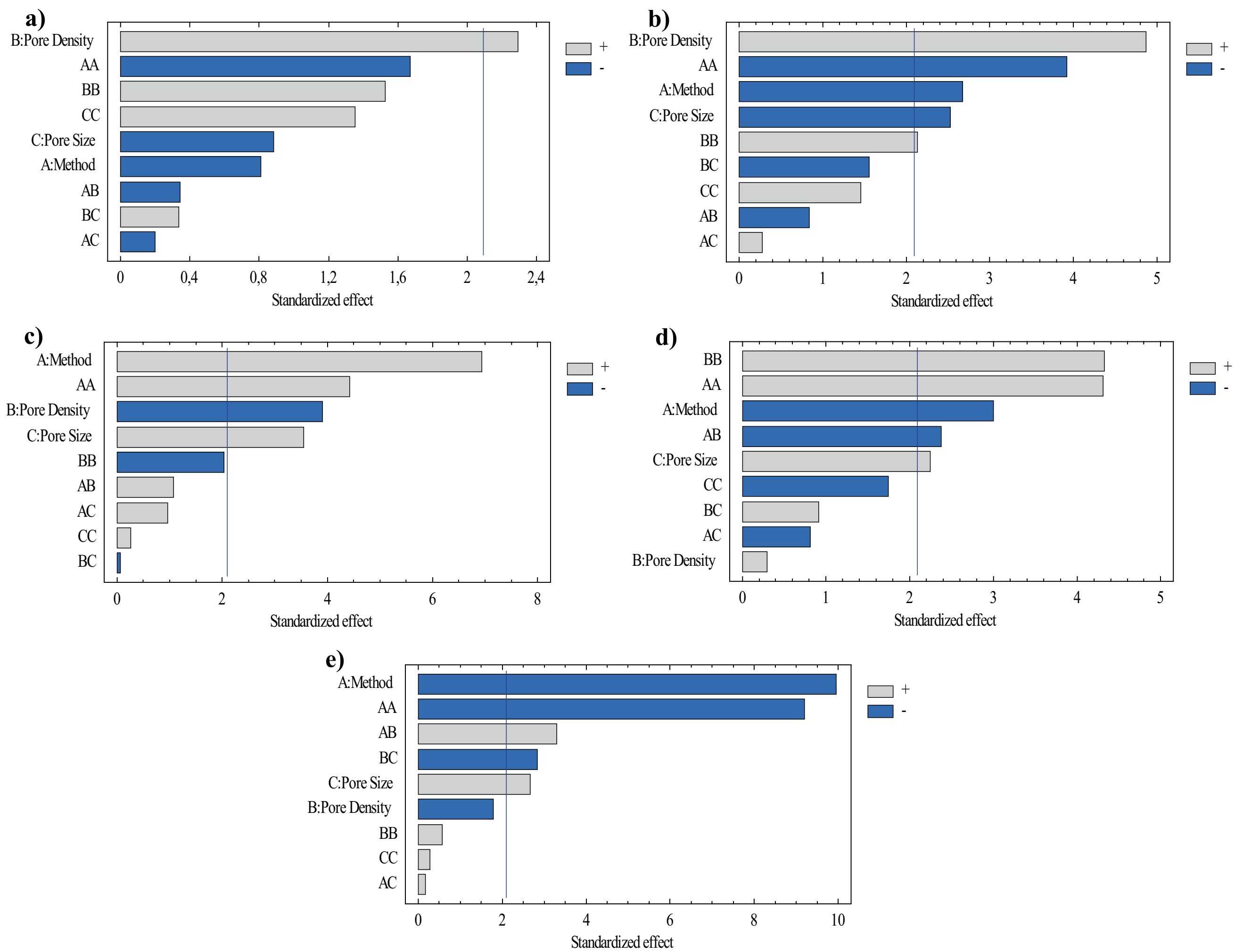

Fig. 3 Standardized Pareto charts (α = 0.05) for **a**) effective diffusivity according to the Fick's second law model, **b**) effective diffusivity according to the anomalous diffusion model, **c**) the alpha value of the anomalous diffusion model, **d**) color change, **e**) soluble solid content

Franco et al. (2019) used an RW™ to dry apples, salmon, and beef and found 50% reductions in treatment time compared with that of CD and color preservation in the final product. Nindo et al. (2003) dehydrated pumpkin puree operating a refractance window with 95 °C water and a belt speed of 2.98 m/min and showed that 80% of the moisture was removed in 1/3 of the CD time; additionally, the final dry product was obtained in 60% of the CD time. Ortiz et al. (2013) reported that salmon slices reached equilibrium in a convective hot air tube at 60 °C for a drying time of 60 h; the time was significantly reduced to 24 h using an RW™ at 55 °C. Various researchers that have studied RW™ dehydration and compared the technique with other methods (e.g., convective drying, spray drying, and freeze-drying) conclude that RW™ drying requires less treatment time and generates better overall product quality (Caparino et al., 2012, 2013; Clarke, 2004; Franco et al., 2019; Nindo & Tang, 2007; Pavan et al., 2012; Rajoriya et al., 2019). These results show the dehydrating effect of energy in the form of radiation from hot water on a portion of food with simple geometry (pulp, liquid, or thin slices) and high humidity. In contrast, the RW™ and CD transmit heat by direct contact at the interface between the water-Mylar® and the Mylar®-food.

Treatments with high PD and large pore size tended to have lower drying time (e.g., experiments 3 (7.94 pores/cm^2, radius of 198 μm), 2 (7.94 pores/cm^2, radius of 300 μm), and 9 (7.94 pores/cm^2, radius of 198 μm) than the control (non-microperforated) drying process (Fig. 4).

Table 4 presents the reduction percentages in relation to the control experiment and shows that the drying method markedly effects the total drying time. OD/CD experiments 1 (radius of 105 μm) and 14 (radius of 300 μm) had the same PD (5.08 pores/cm^2) and the similar drying time (170 and 172.5 min, respectively) but different perforation sizes; thus, the OD/CD method was not affected by the micropore size. Furthermore, experiments 3 and 10 (radius of 198 μm) had different PDs (7.94 and 2.86 pores/cm^2 respectively), which caused slower drying in 14 min approximately (182.5 min vs. 168.8 min) and indicated a possible inverse relationship between drying time and PD (for OD/CD). For OD/RW™ drying, experiments 4 and 12 involved small pores (radius of 105 μm) and the longest drying times (170 min and 163.8 min, respectively), indicating that the variation in PD within this treatment did not significantly affect small pores. However, experiments 2 (7.94 pores/cm^2) and 6 (2.86 pores/cm^2) presented faster drying with larger pore radius (300 μm); experiment 2 had the fastest treatment, indicating that OD/RW™ drying is favored by a high-density of large pores. Experiments 8, 13, and 15 (5.08 pores/cm^2, radius of 198 μm) showed that microperforations favor water movement in OD/RW™ drying (over 19% of reduction). Finally, the longest drying time with LMP (93.3 ± 2.9 min) for RW™ drying was attained under the conditions of experiment 7 (2.86 pores/cm^2, radius of 198 μm), which had the lowest PD and an intermediate pore size (53% reduction). These results indicated a favorable relationship between reduced drying time and increased PD regardless of size, as confirmed by other experiments dried by a RW™ that achieved reductions between 59 and 61%. The greatest reductions in drying time were generally observed in experiments 3, 2, and 5–9 for the OD/CD, OD/RW™, and RW™ treatments, respectively, which mostly had the highest PD (7.94 pores/cm^2).

Fig. 4 Fick's second law model and anomalous diffusion model fittings for the experiments with larger pore densities and the highest time reductions. **A)** Control OD/CD-non-microperforated; **B)** Exp 3 (OD/CD, 7.94 pores/cm^2, radius of 198 μm); **C)** Control OD/RW-non-microperforated; **D)** Exp 2 (OD/RW™, 7.94 pores/cm^2, radius of 300 μm); **E)** Control RW™- non-microperforated; **F)** Exp 9 (RW™, 7.94 pores/cm^2, radius of 198 μm). (This graph only shows the drying stage without considering the previous OD time.)

Effective Moisture Diffusion Coefficient Determination via the Fick's Second Law and Anomalous Models

Table 5 shows the general fitting of the drying data to the two diffusive models of interest. Both fittings yielded admissible coefficients of determination and errors close to zero, which indicated good fittings of the experimental data to the analyzed models with and without laser microperforations. However, the fittings improved with the anomalous diffusion model because of the incorporation of an additional parameter in the equation. Figure 4 presents the drying curves for the microperforated and non-microperforated samples dried with OD/CD, OD/RW™ and, a RW™ and it respective fit to both mathematical models. Microperforation reduced the drying time compared with non-microperforated samples for all drying methods. The drying curves did not show "breaks," suggesting that pore closing caused by shrinkage

Table 4 Drying time reduction at 70 °C for all treatments, including the experiments without laser microperforations

			Time (min)				
		Experiment	OD	CD	RW	Total	%Reduction
OD/CD	No LMP (Control)		95	102,5 ± 3,5^{a}	–	197,5 ± 3,5^{a}	–
	1	(5.08 pores/cm^2, 105 μm)	85	85,0 ± 7,1^{bcde}	–	170 ± 7,1^{bcde}	14
	3	(7.94 pores/cm^2, 198 μm)	85	83,8 ± 2,5^{cde}	–	168,8 ± 2,5^{cde}	15
	10	(2.86 pores/cm^2, 198 μm)	80	102,5 ± 3,5a	–	182,5 ± 3.5^{a}	8
	14	(5.08 pores/cm^2, 300 μm)	82,5	90,0 ± 7,1^{bc}	–	172,5 ± 7,1^{bc}	13
OD/RW™	No LMP		95	–	100,0 ± 7,1^{a}	195,0 ± 7,1^{a}	1
	2	(7.94 pores/cm^2, 300 μm)	77,5	–	76,7 ± 2,9^{ef}	154,2 ± 2,9^{ef}	22
	4	(7.94 pores/cm^2, 105 μm)	82,5	–	87,5 ± 3,5^{bcd}	170,0 ± 3,5^{bcd}	14
	6	(2.86 pores/cm^2, 300 μm)	77,5	–	81,3 ± 7,5^{cdef}	158,8 ± 7,5^{cdef}	20
	8	(5.08 pores/cm^2, 198 μm)	80	–	77,5 ± 3,5^{ef}	157,5 ± 3,5^{ef}	20
	12	(2.86 pores/cm^2, 105 μm)	85	–	78,8 ± 6,3^{def}	163,8 ± 6,3^{def}	17
	13	(5.08 pores/cm^2, 198 μm)	75	–	80,0 ± 5,0^{def}	155,0 ± 5,0^{def}	22
	15	(5.08 pores/cm^2, 198 μm)	80	–	80,0 ± 5,0^{def}	160,0 ± 5,0^{def}	19
RW™	No LMP		–	–	102,5 ± 3,5^{a}	102,5 ± 3,5^{a}	48
	5	(5.08 pores/cm^2, 105 μm)	–	–	73,3 ± 2,9^{f}	73,3 ± 2,9^{f}	63
	7	(2.86 pores/cm^2, 198 μm)	–	–	93,3 ± 2,9^{ab}	93,3 ± 2,9^{ab}	53
	9	(7.94 pores/cm^2, 198 μm)	–	–	80,0 ± 3,5^{def}	80,0 ± 3,5^{def}	59
	11	(5.08 pores/cm^2, 300 μm)	–	–	77,5 ± 2,9^{ef}	77,5 ± 2,9^{ef}	61

Means with different superscripts within a column differ significantly ($p < 0.05$)

LMP Laser microperforations, *OD* Osmotic dehydration, *CD* Conventional drying, *RW* Refractance window

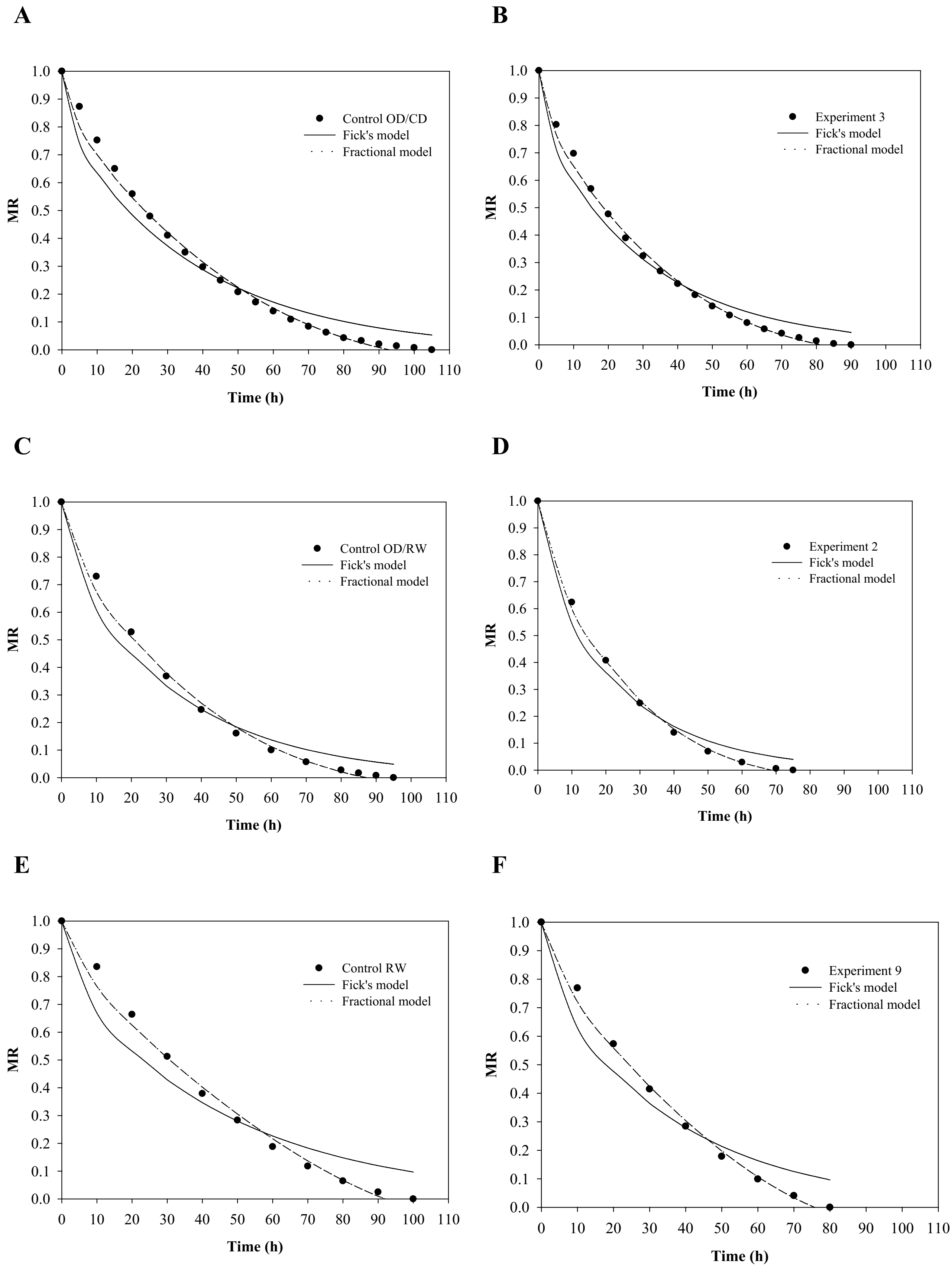
A
Control OD/CD
Fick's model
Fractional model
MR
Time (h)
B
Experiment 3
Fick's model
Fractional model
MR
Time (h)
C
Control OD/RW
Fick's model
Fractional model
MR
Time (h)
D
Experiment 2
Fick's model
Fractional model
MR
Time (h)
E
Control RW
Fick's model
Fractional model
MR
Time (h)
F
Experiment 9
Fick's model
Fractional model
MR
Time (h)

could not have affected water release. Therefore, the time reduction could be explained by micropores that likely favored water migration during the early drying stages. For extended drying times, the inevitable shrinkage of the apple slices promoted micropore collapse and reduced the effect on the water migration rate. The results presented by Fernandez et al. (2005) show that apple shrinkage (through area measurement) was produced smoothly during the first 50% of drying time (6 h) and remained constant until the end of drying with a size area reduction from 4.5 to 2 cm^2 (approximately 56%). A similar proportion of shrinkage also occurs at the microstructural level (Mayor et al., 2005). Therefore, pore size was expected to be reduced by 56% but not wholly closed, allowing water release during at least 50% of the drying time. Table 5 presents the results of the effective diffusion values, which show that the Fickian diffusion coefficients (D_{eff}) of water in apple slices dehydrated at 70 °C by the three drying methods varied from 5.76×10^{-10} to 11.07×10^{-10} m^2/s, depending on the experimental conditions. These values are consistent with those reported by Franco et al. (2019)–Fickian D_{eff} values from 0.61×10^{-10} to 7.32×10^{-10} m^2/s for apple slices dried with CD and 1.25×10^{-10} to 14.30×10^{-10} m^2/s with RW™ methods at 55 °C and 95 °C, respectively. In similar studies, results were 0.62×10^{-9} m^2/s to 3.50×10^{-9} m^2/s for orange slices (Rafiee et al., 2010); 3.16×10^{-10} to 7.68×10^{-10} m^2/s for papaya puree slices (Ocoró-Zamora & Ayala-Aponte, 2013); 2.53×10^{-7} m^2/s for lucuma pulp (Gamboa et al., 2014) 6.75×10^{-10} to 1.28×10^{-9} m^2/s for apple slices (Beigi, 2016) and 1.20×10^{-9} to 3.55×10^{-9} m^2/s for jujube slices (Elmas et al., 2019). These results were consistent with the D_{eff} common range for food materials, with orders of magnitude from 1×10^{-12} to 1×10^{-9} m^2/s (Özkan-Karabacak et al., 2020). Experiments with and without LMP showed that micropores tend to increase the value of D_{eff} due to geometrical modification, because the presence of pores decreases the average distance that the water must travel from the inside of the apple slices to the surface and accelerates the diffusion process.

The highest Fickian diffusion coefficient values were obtained with the OD/RW™ drying method in experiments 2 (7.94 pores/cm^2, radius of 300 μm) and 4 (7.94 pores/cm^2, radius of 105 μm), which had the highest PD and the largest and smallest pore size, respectively. A similar trend

Table 5 Effective diffusion coefficients for all experiments dried at 70 °C, including the experiments without laser microperforations, according to the Fick's second law and anomalous diffusion models

			Fick's second law model			Anomalous diffusion model			
		Experiment	*Deff* 10^{-10} (m2/s)	R^2	*SSE*10^{-2}	*Deff** 10^{-10} (m2/s)	α	R^2	SSE10^{-2}
OD/CD	No LMP (Control)		7.03 ± 0.88*	0.959	7.94	1.33 ± 0.06*	1.20 ± 0.001*	0.993	1.264
	1	(5.08 pores/cm^2, 100 μm)	7.84 ± 0.05^{bcd}	0.97	4.98	1.84 ± 0.03^{cd}	1.18 ± 0.002^{bcd}	0.996	0.597
	3	(7.94 pores/cm^2, 200 μm)	8.57 ± 0.14^{de}	0.973	4.25	2.29 ± 0.56^{d}	1.16 ± 0.029^{bc}	0.997	0.544
	10	(2.86 pores/cm^2, 200 μm)	6.94 ± 0.27^{ab}	0.963	6.71	1.24 ± 0.07^{bc}	1.21 ± 0.002^{cd}	0.997	0.48
	14	(5.08 pores/cm^2, 300 μm)	7.08 ± 0.07^{abc}	0.955	7.99	1.11 ± 0.02^{abc}	1.23 ± 0.002^{cd}	0.994	1.097
OD/RW™	No LMP		8.02 ± 0.46*	0.969	3.62	1.82 ± 0.21*	1.18 ± 0.005*	0.995	0.574
	2	(7.94 pores/cm^2, 300 μm)	10.88 ± 0.53^{f}	0.983	1.58	3.39 ± 0.35^{e}	1.14 ± 0.008^{b}	0.999	0.128
	4	(7.94 pores/cm^2, 100 μm)	11.07 ± 0.68^{f}	0.995	0.5	5.94 ± 0.71^{f}	1.07 ± 0.008^{a}	1	0.021
	6	(2.86 pores/cm^2, 300 μm)	7.27 ± 0.60^{abc}	0.945	5.81	0.70 ± 0.36^{ab}	1.30 ± 0.055^{e}	0.993	0.718
	8	(5.08 pores/cm^2, 200 μm)	9.32 ± 1.52^{e}	0.965	3.65	1.77 ± 1.12^{cd}	1.22 ± 0.065^{cd}	0.997	0.321
	12	(2.86 pores/cm^2, 100 μm)	8.36 ± 0.51^{cde}	0.966	3.5	1.36 ± 0.41^{bcd}	1.22 ± 0.030^{cd}	0.998	0.18
	13	(5.08 pores/cm^2, 200 μm)	9.31 ± 0.44^{e}	0.972	2.87	2.07 ± 0.32^{cd}	1.19 ± 0.012^{bcd}	0.998	0.245
	15	(5.08 pores/cm^2, 200 μm)	8.72 ± 0.40^{de}	0.965	3.29	1.31 ± 0.17^{bcd}	1.23 ± 0.010^{d}	0.998	0.153
RW™	No LMP		5.77 ± 0.20*	0.928	8.44	0.34 ± 0.06*	1.35 ± 0.002*	0.991	1.061
	5	(5.08 pores/cm^2, 100 μm)	7.52 ± 0.27^{abcd}	0.943	5.62	0.60 ± 0.06^{ab}	1.31 ± 0.007^{e}	0.995	0.506
	7	(2.86 pores/cm^2, 200 μm)	6.46 ± 0.41^{a}	0.942	7.03	0.53 ± 0.02^{ab}	1.30 ± 0.000^{e}	0.996	0.559
	9	(7.94 pores/cm^2, 200 μm)	7.17 ± 0.33^{abc}	0.944	5.36	0.55 ± 0.12^{ab}	1.32 ± 0.024^{e}	0.996	0.412
	11	(5.08 pores/cm^2, 300 μm)	6.22 ± 0.07^{a}	0.924	8.13	0.21 ± 0.02^{a}	1.42 ± 0.012^{f}	0.995	0.54

Means with different superscripts within a column differ significantly ($p < 0.05$)

LMP Laser microperforations, *OD* Osmotic dehydration, *CD* Conventional drying, *RW* Refractance window, D_{eff} Effective diffusion coefficient (m^2/s), D_{eff}^* Effective anomalous diffusion coefficient (m^2/s^{α}), R^2 Coefficient of determination, *SSE* Sum of squared errors, *α* Alpha value

*corresponds to each drying method without laser microperforations was observed for the other drying methods, where the treatments with the highest number of microperforation tended to present the highest Fickian D_{eff} values (experiments 3 and 9 with 7.94 pores/cm^2). These results confirmed the directly proportional influence of PD on diffusion based on the Fick's second law (Fig. 3a and Table 3).

On the one hand, the results of the anomalous diffusion model showed that D_{eff}* increased with PD; the highest D_{eff}* values were obtained at the highest PD (Fig. 3b). On the other hand, the drying method also affected the value of D_{eff}*. For OD/CD and OD/RW™ drying, D_{eff}* values ranged from 1.11×10^{-10} to 2.29×10^{-10} m^2/s$^\alpha$ and 0.70×10^{-10} to 5.94×10^{-10} m^2/s$^\alpha$, respectively. For RW™ drying, D_{eff}* values ranged from 0.21×10^{-10} to 0.60×10^{-10} m^2/s–significantly lower than those of the other two methods.

Figure 5 shows the abovementioned behaviors and depicts the surface graphic for Fick's second law and anomalous diffusion as a function of PD and size. Notably, the PD factor positively affected the response variable with curvature (Fig. 5a), indicating a non-linear correlation; additionally, the PS factor had less influence on the Fickian coefficient. Likewise, a positive effect and more linear relationship between the PD variable and the anomalous diffusion coefficient was confirmed. The relationship between the PS and the anomalous diffusion coefficient is semi-linear and inversely proportional.

Table 5 shows that α ranged between 1.07 and 1.42 thus indicating a super-diffusive behavior (α > 1) for water through and outside the apple. Rajoriya et al. (2019) obtained similar results and concluded that the nature of the diffusion process during apple slice drying showed super-diffusive behavior (α > 1). The α parameter is associated with the microstructural characteristics of the food matrix and remains constant as long as the microstructure remains invariable. LMPs do not count as microstructural modifications but shorten the distance that the water must travel through the tissue. Analysis of the α value results shows that values that remain similar tend to vary according to the type of drying method and the perforations (Fig. 3c). Therefore, the effect of pores on food geometry is reflected in the alpha value even if neglected by the mathematical model. Thus, the obtained *α* value is more similar to *α′*; this result is somewhat similar to the case of the effective diffusion coefficient, which is used because diffusion does not usually occur independently. Therefore, D_{eff} covers several of the phenomena that occur in the process and is easier to estimate (Gómez et al., 2015; Segura-Ponce et al., 2019). Many different mechanisms occur at the pore level and at different stages of drying, the relative importance of which depends on the drying conditions, pore topology, pore geometry, and wall composition of the porous medium (Segura-Ponce et al., 2019). This position is based on research that found

Fig. 5 Surface response of the effects of pore size and pore density on the diffusion coefficients of apple slices dried at 70 °C via the OD/RW™ method fitted through **a**) Fick's second law model and **b**) the anomalous diffusion model

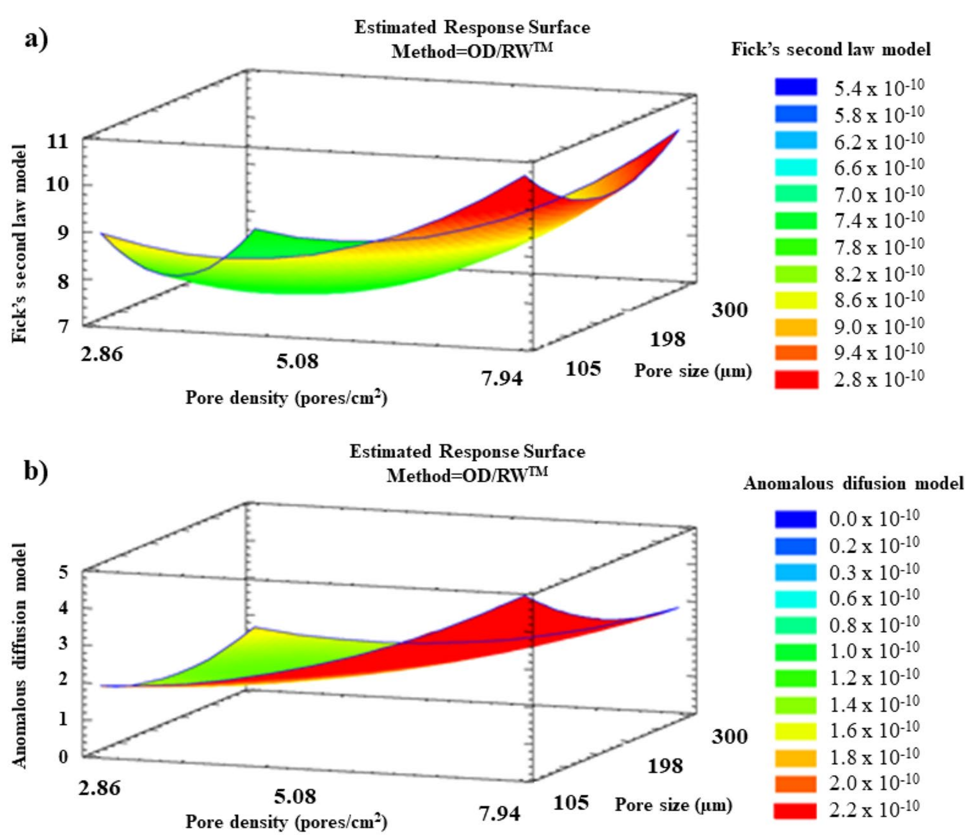

that the food matrix was subjected to temperature variations but not changes in geometry, resulting in constant α values (Ramírez et al., 2017; Simpson et al., 2015).

RW™ drying generally presented α values (1.3–1.41) significantly higher than those obtained using OD/RW™ drying and OD/CD. This suggests that super-diffusive behavior prevails over the other mechanism which is attributed to longer jumps by water molecules through the apple matrix caused by a faster evaporation promoted by refractance window radiation. Similar behavior was presented in apple slices dried using RW™ by Franco et al. (2019) and Hernández et al. (2019).

Microstructural heterogeneity, shrinkage phenomena, and water distribution prevent the adequate fitting of food material to the Fick's second law model. Effectively, the food material remains in a rubbery state throughout the process (Kurazawa et al., 2012). However, the structural collapse closes the water path and slows water movement (Saravacos & Maroulis, 2001). The application of the anomalous model in food dehydration has been mentioned previously by Simpson et al. (2013), Simpson et al. (2015), Ramírez et al. (2017) and Rajoriya et al., (2019a, b). This non-Fickian model is used to evaluate alternatives to the traditional model that include the anomalous diffusion model based on fractional calculus. The fractional calculus approach converges to a Fickian behavior for a fractional order of 1. Because the value obtained is significantly different, the Fickian approach does not represent the diffusion in the system. Thus, the use of the anomalous diffusion model is validated.

Quality Analysis

Table 6 shows the values obtained for the coordinates of the CIEL*a*b* color space and the magnitude of color change (ΔE) compared to the fresh apple and drying performed without LMP at 70 °C. Conventionally dried samples (OD/CD) deliver ΔE values (6.88–13.40) comparable to those reported by similar studies of GS apples under air drying (e.g., Moreno et al., 2016). These authors report values of 10.63, 12.33, and 7.72 for samples dried at 50 °C, 60 °C, and 70 °C, respectively, without any pre-treatment.

The fresh apple slices had values of $L^* = 73.10 \pm 1.67$, $a^* = -6.76 \pm 1.58$, $b^* = 17.57 \pm 3.35$, and 11.65% SS, indicating that the drying conditions (70 °C) of the three evaluated methods significantly affected the ΔE parameter and soluble solids content (Fig. 3d, e) ($p < 0.05$). Similar results were obtained from other GS apple drying investigations (Franco et al., 2019; Hernández et al., 2019; Moreno et al., 2013, 2016; Ramírez et al., 2017; Schulze et al., 2012; Segura-Ponce et al., 2019; Tavera-Quiroz, et al., 2014; Vega-Gálvez et al., 2012). Experiments with no LMP presented $\Delta E_{(\text{fresh apple})}$ values between 12.94 and 14.40, which correspond to changes perceptible to the naked eye. The same results were observed in all treatments with microperforations, with ΔE values between 6.88 and 11.63. However, after microperforation, the magnitude of the $\Delta E_{(\text{fresh apple})}$ values for all drying methods decreased. Therefore, laser pre-treatment affects the magnitude of the change in color of the dry samples compared to that of the fresh apple, indicating less color degradation due to a heat and mass transfer facilitated by the effect of the holes in the sample and a shorter drying time. Pathare et al. (2013) state that color is an indicator of the severity of heat treatment and helps to predict quality deterioration caused by heat exposure. The results of only the effect of microperforations on color changes during drying reveal lower values of $\Delta E_{(\text{method without LMP})}$. For example, the smallest microperforations (104.90 µm) tend to lead to a smaller ΔE (e.g., in treatments 1 (5.08 pores/cm^2), 4 (7.94 pores/cm^2), 12 (2.86 pores/cm^2), and 5 (5.08 pores/cm^2), with values of 4.53, 4.12, 5.71, and 5.06, respectively, that are barely perceptible to the human eye).

Significant differences in the effects on color change of the drying methods could not be identified, because all the methods favor enzymatic browning. However, average ΔE values tend to decrease when using RW™ drying with or without OD pre-treatment compared to those of conventionally dried samples (OD/CD method). OD/RW™ drying had the lowest $\Delta E_{(\text{method without LMP})}$ average values (4.99), followed by RW™ drying (5.81) and OD/CD (7.27), which indicated a favorable effect when drying the samples in the RW™. These results are consistent with those of other investigations of the RW™ drying method technology, which has demonstrated potential for drying fruits and vegetables at temperatures between 55 °C and 96 °C and for reducing drying times at different temperature levels with the same or less impact on the final quality. Additionally, RW methods preserve bioactive compounds, color, and flavor and reduces microbial activity (Raghavi et al., 2018; Sabarez, 2019).

Table 6 shows the soluble solid content results. All the solids concentrations in the samples increased significantly due to water loss during drying and to mechanisms of mass and heat transfer, with and without LMP ($p < 0.05$). The smallest increase in SS occurred in drying by RW™ drying (average of 562%) compared to OD/CD and OD/RW drying (averages of 669% and 701%, respectively). This result was expected, because the RW™ samples were not pretreated with OD; therefore, no additional solids were incorporated into the samples from the osmotic solution. Garcia et al. (2013) reported that the many advantages of OD include better retention of color and flavor and low energy requirement. However, the abovementioned results reinforce the idea that the RW™ is advantageous, because it obtains dry samples in less time with less quality reductions and low

Table 6 Mean values of soluble solids and color parameters for fresh apple and all treatments dried at 70 °C, including the experiments without laser microperforations

	Experiment		SS (%)	ΔE (fresh apple)	ΔE (Method without LMP)
	Fresh		11.65 ± 1.83**	0.00 ± 0.00**	–**
OD/CD	No LMP (Control)		69.89 ± 0.83*	13.40 ± 1.06*	0.00 ± 0.00*
	1	(5.08 pores/cm², 100 μm)	79.81 ± 0.10^{f}	9.99 ± 1.33^{de}	4.53 ± 1.64^{ab}
	3	(7.94 pores/cm², 200 μm)	73.23 ± 0.70^{d}	6.88 ± 1.47^{a}	10.60 ± 1.45^{f}
	10	(2.86 pores/cm², 200 μm)	83.23 ± 0.72^{h}	7.62 ± 1.54^{ab}	7.65 ± 1.20^{e}
	14	(5.08 pores/cm², 300 μm)	83.55 ± 1.24^{h}	10.34 ± 1.25^{def}	6.31 ± 1.81^{de}
OD/RW™	No LMP		75.31 ± 1.28*	12.94 ± 0.84*	0.00 ± 0.00*
	2	(7.94 pores/cm², 300 μm)	81.77 ± 0.69^{g}	9.87 ± 0.62^{de}	5.72 ± 1.77^{bcd}
	4	(7.94 pores/cm², 100 μm)	84.02 ± 0.79^{h}	9.69 ± 1.39^{d}	4.12 ± 1.22^{a}
	6	(2.86 pores/cm², 300 μm)	89.22 ± 2.12^{j}	8.33 ± 0.67^{bc}	6.06 ± 1.28^{cd}
	8	(5.08 pores/cm², 200 μm)	82.38 ± 0.64^{h}	9.94 ± 0.79^{de}	4.61 ± 1.83^{abc}
	12	(2.86 pores/cm², 100 μm)	78.91 ± 0.07^{f}	11.63 ± 0.94^{g}	5.71 ± 1.74^{bcd}
	13	(5.08 pores/cm², 200 μm)	77.71 ± 0.80^{e}	11.38 ± 0.60^{fg}	4.61 ± 1.97^{abc}
	15	(5.08 pores/cm², 200 μm)	84.37 ± 3.37^{i}	10.58 ± 1.16^{defg}	4.14 ± 1.41^{a}
RW™	No LMP		62.53 ± 0.68*	14.41 ± 0.87*	0.00 ± 0.00*
	5	(5.08 pores/cm², 100 μm)	61.40 ± 0.73^{a}	10.95 ± 1.39^{efg}	5.06 ± 1.85^{abcd}
	7	(2.86 pores/cm², 200 μm)	67.12 ± 0.67^{b}	10.31 ± 1.15^{def}	6.37 ± 1.20^{de}
	9	(7.94 pores/cm², 200 μm)	69.90 ± 1.28^{c}	9.43 ± 1.36^{cd}	5.96 ± 1.39^{bcd}
	11	(5.08 pores/cm², 300 μm)	66.22 ± 0.41^{b}	10.33 ± 2.19^{defg}	5.83 ± 2.65^{bcd}

Means with different superscripts within a column differ significantly ($p < 0.05$)

LMP Laser microperforations, *OD* Osmotic dehydration, *CD* Conventional drying, *RW* Refractance window, *SS* Soluble solid content, *ΔE* Color change

* corresponds to each drying method without laser microperforations; ** corresponds to fresh apple

energy costs. The percentage of solids found in the dehydrated samples is similar to that reported by Hernández et al. (2019) for the drying of GS apples, with values at 55 °C that ranged between 66% of SS for hot air-drying, 73% for RW™ drying, and 80% for osmotically pretreated RW™ drying.

Raghavi et al. (2018) noted that 85% of industrial dryers are convective types that produce inferior quality and require long drying times; nonetheless, RW™ drying can produce high-quality dried products with nutritional attributes. Additionally, Nindo and Tang (2007) produced high-quality dried mango pulp with lower costs and time requirements than products obtained by tray, spray, and freeze-drying. RW™ drying systems cost between 30 and 50% less than freeze dryers and require less than half the energy to dry the same amount of product. As the thermal conductivity of the plastic material is relatively low, little energy is transmitted via conduction from the heated water to the food on the plastic film, reducing the rate of heating and protecting the product color and flavor from degradation due to overheating (Bolland, 2000). Additionally, the window mechanism provides the system with a self-regulation medium via the coupled heat and mass transfer mechanisms (Sabarez, 2019).

Conclusions

RW™ drying without OD pre-treatment showed a significant increase in the mass transfer of apple slices and a 50% reduction in drying time compared to that of the control (with no LMP). These results are relevant when considering the low installation and operating costs of RW™ drying compared to other methods, such as freeze-drying and spray drying. In general, OD pre-treatment reduced drying time for conventional and reflectance window drying as compared with non-pretreated samples. However, the extended OD time did not justify application compared with the time and final color results obtained by RW™ drying.

As expected, more perforations with larger PS accelerated the drying process and obtained higher effective diffusion coefficient values based on Fick's second law. Additionally, fewer color changes and soluble solids were obtained in the final product.

The anomalous diffusion model based on fractional calculus produced better fits for the experimental data with and without LMP and improved the modeling of mass transport through porous media, such as food. Super-diffusive behavior ($\alpha > 1$) was found, where α and D_{eff}^{*} were associated with the microstructural changes and process conditions, respectively.

Acknowledgements The authors are grateful for the financial support provided by CONICYT through FONDECYT project numbers 1181270 and 1191270, the Postgraduate and Programs Management, and the Food Processing and Bioprocess Laboratory of the Department of Chemical and environmental Engineering of the USM.

Funding Fondo Nacional de Desarrollo Científico y Tecnológico, 1181270,Ricardo Simpson,1191280,Cristian Ramírez

Data Availability Data will be made available on reasonable request.

Declarations

Conflict of Interest The authors declare no conflict of interest.

References

Abul-Fadl, M., & Ghanem, T. (2011). Effect of Refractance Window (RW) drying method on quality criteria of produced tomato powders as compared to the convection drying method. *World Applied Sciences Journal, 15*, 953–965.

Ahmad-Qasem, M., Santacatalina, J., Barrajón-Catalán, E., Micol, V., Cárcel, J., & García-Pérez, J. (2015). Influence of Drying on the Retention of Olive Leaf Polyphenols Infused into Dried Apple. *Food and Bioprocess Technology, 8*(1), 120–133. https://doi.org/10.1007/s11947-014-1387-6

AOAC20013. (1980). Official Methods of Analysis. *17th Edition, The Association of Official Analytical Chemists, Gaithersburg, MD, USA*.

Badui D., S. (2006). Química de los alimentos. (4a. ed.). México: Pearson Education. ISBN: 970–26–0670–5.

Beigi, M. (2016). Energy efficiency and moisture diffusivity of apple slices during convective drying. *Food Science and Technology, 36*, 145–150. https://doi.org/10.1590/1678457X.0068

Blutinger, J. D., Meijers, Y., Chen, P. Y., Zheng, C., Grinspun, E., & Lipson, H. (2019). Characterization of CO2 laser browning of dough. *Innovative Food Science and Emerging Technologies, 52*, 145–157. https://doi.org/10.1016/j.ifset.2018.11.013

Bolland, K. M. (2000). A new low-temperature/short-time drying process. *Cereal Foods World, 45*, 293–296.

Caparino, O. A., Sablani, S. S., Tang, J., Syamaladevi, R. M., & Nindo, C. I. (2013). Water sorption, glass transition, and microstructures of Refractance window – And freeze dried mango (Philippine "Carabao" var.) powder. *Drying Technology, 31*, 1969–1978. https://doi.org/10.1080/07373937.2013.805143

Caparino, O. A., Tang, J., Nindo, C. I., Sablani, S. S., Powers, J. R., & Fellman, J. K. (2012). Effect of drying methods on the physical properties and microstructures of mango (Philippine' Carabao' var.) powder. *Journal of Food Engineering, 111*, 135–148. https://doi.org/10.1016/j.jfoodeng.2012.01.010

Clarke, P. T. (2004). Refractance window - "Down under". *Drying - Procedings of the 14th International Drying Symposium (IDS 2004), B*, 813–820. https://www.yumpu.com/en/document/read/15660238/refractance-window-tm-down-under-phillip-tclarke. Accessed: 25 Nov 2020.

Corzo, O., & Bracho, N. (2007). Determination of water effective diffusion coefficient of sardine sheets during vacuum pulse osmotic dehydration. *Food Science and Technology (LWT), 40*, 1452–4158. https://doi.org/10.1016/j.lwt.2006.04.008

Crank, J. (1975). The mathematics of diffusion. *Oxford University Press*.

Duarte-Correa, Y., Díaz-Osorio, A., Osorio-Arias, J., Sobral, P. J. A., & Vega-Castro, O. (2020). Development of fortified low-fat potato chips through vacuum Ipregnation and microwave vacuum drying. *Innovative Food Science and Emerging Technologies, 64*(February).

DUPONT. (2012). Mylar polyester film: Chemical properties. *Dupont teijin film*, 4, 102437. https://doi.org/10.1016/j.ifset.2020.102437

Elmas, F., Varhan, E., & Koç, M. (2019). Drying characteristics of jujube (Zizyphus jujuba) slices in a hot air dryer and physicochemical properties s of jujube powder. *Journal of Food Measurement and Characterization, 13*, 70–86. https://doi.org/10.1007/s11694-018-9920-3

Etxeberria, E., Miller, W., & Achor, D. (2006). Anatomical and morphological characteristics of laser etching depressions for fruit labeling. *HortTechnology, 16*, 527–532.

Fernandes, F., Rodrigues, S., Cárcel, J., & García-Pérez, J. (2015). Ultrasound-assisted air-drying of apple (Malus domestica L.) and Its effects on the vitamin of the dried product. *Food and Bioprocess Technology, 8,* 1503–1511. https://doi.org/10.1007/s11947-015-1519-7

Fernandez, L., Castillero, C., & Aguilera, J. M. (2005). An application of image analysis to dehydration of apple discs. *Journal of Food Engineering, 67,* 185–193. https://doi.org/10.1016/j.jfoodeng.2004.05.070

Ferraz, A., Carlos, O., Mittal, S., Bilanski, K., & Abdullah, A. (2007). Mathematical modeling of laser based potato cutting and peeling. *Bio Systems, 90*, 602–613.

Figueroa, C., Ramírez, C., Núñez, H., Jaques, A., & Simpson, R. (2020). Application of vacuum impregnation and CO2-laser microperforations in the potential acceleration of the pork marinating process. *Innovative Food Science and Emerging Technologies, 66*. https://doi.org/10.1016/j.ifset.2020.102500

Franco, S., Jaques, A., Pinto, M., Fardella, M., Valencia, P., Núñez, H., & Simpson, R. (2019). Dehydration of salmon (Atlantic salmon), beef, and apple (Granny Smith) using Refractance window™: Effect on diffusion behavior, texture, and color changes. *Innovative Food Science & Emerging Technologies, 52,* 8–16. https://doi.org/10.1016/j.ifset.2018.12.001

Fujimaru, T., Ling, Q., & Morrisey, M. T. (2012). Effects of Carbon Dioxide (CO_2) laser perforation as skin pre-treatment to improve sugar infusion process of frozen blueberries. *Journal of Food Science, 77,* E45–E51. https://doi.org/10.1111/j.1750-3841.2011.02525.x

Gallo, G., & L. A., Tirado A., D. F., & Acevedo C., D. (2015). Deshidratación osmótica: Una revisión. *Revisiones De La Ciencia Tecnología e Ingeniería De Los Alimentos (ReCiTeIA), 15*, 1–12.

Gamboa, D., Ibáñez, D., Meléndez, M., Paredes, E., & Siche, R. (2014). Drying of lucuma (Pouteria obovata) using the technique of Refracting WindowTM. *Scientia Agropecuaria, 5*, 103–108. https://doi.org/10.17268/sci.agropecu.2014.02.05

Garcia, L., & A., Guerrero, S., Gomez, P., & Alzamora, S. (2013). Relationships between rheological properties, texture and structure of apple (Granny Smith var.) affected by blanching and/or osmotic dehydration. *Food and Bioprocess Technology, 6*(2), 475–488. https://doi.org/10.1007/s11947-011-0701-9

Gilpavas, E., Medina, J., Dobrosz-Gómez, I., & Gómez, M. A. (2016a). Optimización de los Costos de Operación del Proceso de Electrooxidación para una Planta de Tratamiento de Aguas Mediante Análisis Estadístico de Superficie de Respuesta. *Información Tecnológica, 27*, 73–82. https://doi.org/10.4067/S0718-07642016000400008

Gilpavas, E., Medina, J., Dobrosz-Gómez, I., & Gómez, M. A. (2016b). Degradación de Colorante Amarillo 12 de Aguas Residuales Industriales utilizando Hierro Cero Valente, Peróxido de Hidrógeno y Radiación Ultravioleta. *Información Tencológica, 27*, 23–34. https://doi.org/10.4067/S0718-07642016000300004

Gómez S. J. A., Clemente P. G., & Sanjuán P. N. (2015). Review of mathematical models to describe the food salting process. *DYNA Universidad Nacional de Colombia*, 23-30. https://doi.org/10.15446/dyna.v82n190.42016

Gutiérrez P. H., & De la Vara S. R. (2008). *Análisis y diseño de experimentos* (Segunda ed.). México D.F.: Cámara Nacional de la Industria Editorial Mexicana.

Heras-Ramírez, M., Quintero-Ramos, A., Camacho-Dávila, A., Bamard, J., Talamás-Abbud, R., Torres-Muñoz, J., & Salas-Muñoz, E. (2012). Effect of Blanching and Drying Temperature on Polyphenolic Compound Stability and Antioxidant Capacity of Apple Pomace. *Food and Bioprocess Technology, 5*(6), 2201–2210. https://doi.org/10.1007/s11947-011-0583-x

Hernández, Y., Ramírez, C., Moreno, J., Núñez, H., Vega, O., Almonacid, S., Pinto, M., Fuentes, L., Simpson, R. (2019). Effect of Refractance Window on dehydration of osmotically pretreated apple slices: Color and texture evaluation. *Journal of Food Process Engineering*, 1-11. https://doi.org/10.1111/jfpe.13304

Jaramillo, A. C., Echavarría, A. M., & Hormaza, A. (2013). Diseño Box-Behnken para la optimización de la adsorción del colorante azul ácido sobre residuos de flores. *Ingeniería y Ciencia, 9*, 75–91. https://doi.org/10.17230/ingciecia.9.18.4

Kaspar, K., Park, J., Mathison, B., & Boon, P. (2012). Processing of pigmented-flesh potatoes (Solanum tuberosum L.) on the retention of bioactive compounds. *International Journal of Food Science & Technology, 47*, 376–382. https://doi.org/10.1111/j.1365-2621.2011.02850.x

Kahraman, O., Malvandi, A., Vargas, L., & Feng, H. (2021). Drying characteristics and quality attributes of apple slices dried by a non-thermal ultrasonic contact drying method. *Ultrasonics Sonochemistry, 73*, 105510. https://doi.org/10.1016/j.ultsonch.2021.105510

Kurazawa, L. E., Dupas, M., & Park, K. J. (2012). Glass transition phenomenon on shrinkage of papaya during convective drying. *Journal of Food Engineering, 108*, 43–50. https://doi.org/10.1016/j.jfoodeng.2011.07.033

Landl, A., Abadias, M., Sárraga, C., Viñas, I., & Picouet, P. A. (2010). Effect of high pressure processing on the quality of acidified Granny Smith apple purée product. *Innovative Food Science and Emerging Technologies, 11*, 557–564. https://doi.org/10.1016/j.ifset.2010.09.001

Lewicki, P. P., & Jakubczyk, E. (2004). Effect of hot air temperature on mechanical properties of dried apples. *Journal of Food Engineering, 64*, 307–314. https://doi.org/10.1016/j.jfoodeng.2003.10.014

Lewicki, P. P., & Lukaszuk, A. (2000). Changes of rheological properties of apple tissue undergoing convective drying. *Drying Technology, 18*, 707–722. https://doi.org/10.1080/07373930008917733

Magoon, R. (1986). Method and apparatus for drying fruit pulp and the like. *US Patent 4631837*.

Mayor, L., Silva, M. A., & Sereno, A. M. (2005). Microstructural Changes during Drying of Apple Slices. *Drying Technology, 23*, 2261–2276.

Menon, A., Stojceska, V., & Tassou, S. A. (2020). A systematic review on the recent advances of the energy efficiency improvements in non-conventional food drying technologies. *Trends in Food Science & Technology, 100*, 67–76. https://doi.org/10.1016/j.tifs.2020.03.014

Mohapatra, D., Mishra, S., Singh, C., & Singh, D. (2011). Post-harvest Processing of Banana: Opportunities and Challenges. *Food Bioprocess Technology, 4*, 327–339. https://doi.org/10.1007/s11947-010-0377-6

Montoya, J. E. Z., & Quintero, G. C. (1999). Deshidratación osmótica de frutas y vegetales. *Revista Facultad Nacional De Agronomía Medellín, 52,* 451–466.

Moraga, G., Talens, P., Moraga, M. J., & Martínez-Navarrete, N. (2011). Implication of water activity and glass transition on the mechanical and optical properties of freeze-dried apple and banana slices. *Journal of Food Engineering, 106*(3), 212–219. https://doi.org/10.1016/j.jfoodeng.2011.05.009

Moreno, J., Espinoza, C., Simpson, R., Petzold, G., Nuñez, H., & Gianelli, M. P. (2016). Application of ohmic heating/vacuum impregnation treatments and air drying to develop an apple snack enriched in folic acid. *Innovative Food Science & Emerging Technologies, 33*, 381–386. https://doi.org/10.1016/j.ifset.2015.12.014

Moreno, J., Simpson, R., Pizarro, N., Pavez, C., Dorvil, F., Petzold, G., & Bugueño, G. (2013). Influence of ohmic heating/osmotic dehydration treatments on polyphenoloxidase inactivation, physical properties and microbial stability of apples (cv. Granny Smith). *Innovative Food Science and Emerging Technologies*, 1-10. https://doi.org/10.1016/j.ifset.2013.06.006

Munzenmayer, P., Ulloa, J., Pinto, M., Ramírez, C., Valencia, P., Simpson, R., & Almonacid, S. (2020). Freeze-drying of blueberries: Effects of carbon dioxide (CO_2) laser perforation as skin pre-treatment to improve mass transfer, primary drying time and quality. *Foods, 9*, 1–18. https://doi.org/10.3390/foods9020211

Nindo, C. I., & Tang, J. (2007). Refractance window dehydration technology: A novel contact drying method. *Drying Technology, 25*, 37–48. https://doi.org/10.1016/j.lwt.2006.07.006

Nieto, A. B., Vicente, S., Hodara, K., Castro, M. A., & Alzamora, S. M. (2013). Osmotic dehydration of apple: Influence of sugar and water activity on tissue structure, rheological properties and water mobility. *Journal of Food Engineering, 119*(1), 104–114. https://doi.org/10.1016/j.jfoodeng.2013.04.032

Nindo, C., Sun, T., Wang, S., Tang, J., & Powers, J. (2003). Evaluation of drying technologies for retention of physical quality and antioxidants in asparagus (Asparagus officinales, L.). *LWT - Lebensm Wiss Technolog, 36*, 507–516. https://doi.org/10.1016/S0023-6438(03)00046-X

Nindo, C., Feng, H., Shen, G., Tang, J., & Kang, D. (2003). Energy utilization and microbial reduction in a new film drying system. *Journal of Food Processing and Preservation, 27*, 117–136. https://doi.org/10.1111/j.1745-4549.2003.tb00506.x

Ochoa-Martínez, C. I., Quintero, P. T., Ayala, A. A., & Ortiz, M. J. (2012). Drying characteristics of mango slices using the Refractance Window™ technique. *Journal of Food Engineering, 109*, 69–75. https://doi.org/10.1016/j.jfoodeng.2011.09.032

Ocoró-Zamora., M. U., & Ayala-Aponte, A. A. (2013). Influence of thickness on the drying of papaya puree (Carica papaya L.) through refractance windowTM technology. *DYNA., 80*, 147–154.

Olivares, J., Nunez, H., Ramírez, C., Jaques, A., Pinto, M., Fuentes, L., Almonacid, S., Vega-Castro, O., & Simpson, R. (2021). Application of moderate electric fields and CO2-laser microperforations for the acceleration of the salting process of atlantic salmon (salmo salar). *Food and Bioproduct Processing, 125*, 105–112. https://doi.org/10.1016/j.fbp.2020.10.014

Ortiz, J., Lemus-Mondaca, R., Vega-Galvez, A., Ah-Hen, K., Puente-Díaz, L., Zura-Bravo, L., & Aubourg, S. (2013). Influence of air-drying temperature on drying kinetics, colour, firmness and biochemical characteristics of Atlantic salmon (Salmo salar L.). *Food Chemistry, 139*, 162–169. https://doi.org/10.1016/j.foodchem.2013.01.037

Özkan-Karabacak, A., Acoglu, B., Yolci Ömeroglu, P., & Çopur, O. U. (2020). Microwave pre-treatment for vacuum drying of orange slices: Drying characteristics, rehydration capacity and quality properties. *Journal of Food Process Engineering*, 1-15. https://doi.org/10.1111/jfpe.13511

Pathare, P., Opara, U., & Al-Said, F. (2013). Colour Measurement and Analysis in Fresh and Processed Foods: A Review. *Food Bioprocess Technology, 6*, 36–60. https://doi.org/10.1007/s11947-012-0867-9

Pavan, M. A., Schmidt, S. J., & Feng, H. (2012). Water sorption behavior and thermal analysis of freeze-dried, Refractance Window-dried and hot-air dried açaí (Euterpe oleracea Martius) juice. *LWT - Food Science and Technology, 48*, 75–81. https://doi.org/10.1016/j.lwt.2012.02.024

Puente-Díaz, L., Spolmann, O., Nocetti, D., Zura-Bravo, L., & Lemus-Mondaca, R. (2020). Effects of Infrared-Assisted Refractance Window™ Drying on the Drying Kinetics, Microstructure, and

Color of *Physalis* Fruit Purée. *Foods, 9*, 343. https://doi.org/10.3390/foods9030343

Rajoriya, D., Shewale, S. R., & Hebbar, H. U. (2019). Refractance window drying of apple slices: Mass transfer phenomena and quality parameters. *Food and Bioprocess Technology, 12,* 1646–1658. https://doi.org/10.1007/s11947-019-02334-7

Rafiee, S., Sharifi, M., Kayhani, A., Omid, M., Jafari, A., Mohtasebi, S. S., & Mobli, H. (2010). Modeling effective moisture diffusivity of orange slice (Thompson Cv.). *International Journal of Food Properties, 13*, 32–40. https://doi.org/10.1080/10942910802144345

Raghavi, L. M., Moses, J. A., & Anandharamakrishnan, C. (2018). Refractance window drying of foods: A review. *Journal of Food Engineering, 222*, 267–275. https://doi.org/10.1016/j.jfoodeng.2017.11.032

Ramírez, C., Astorga, V., Núñez, H., Jaques, A., & Simpson, R. (2017). Anomalous diffusion based on fractional calculus approach applied to drying analysis of apple slices: The effects of relative humidity and temperature. *Food Process Engineering*, 1-10. https://doi.org/10.1111/jfpe.12549

Ramírez, N., Vega-Castro, O., Simpson, R., Ramírez, C., & Nunez, H. (2021). Effect of pulsed vacuum and laser microperforations on the potential acceleration of chicken meat marination. *Journal of Food Process Engineering, 44*, 13627. https://doi.org/10.1111/jfpe.13627

Sabarez, H. (2019). Refractance Window™ Drying: A Mechanistic Understanding of the Drying Process Using Modelling Approach. *Reference Module in Food Science*. https://doi.org/10.1016/B978-0-08-100596-5.21439-X

Saravacos, G., & Maroulis, Z. (2001). *Transport properties of foods*. Marcel Dekker, Inc.

Schulze, B., Peth, S., Hubbermann, E. M., & Schwarz, K. (2012). The influence of vacuum impregnation on the fortification of apple parenchyma with quercetin derivatives in combination with pore structures X-ray analysis. *Journal of Food Engineering, 109*, 380–387. https://doi.org/10.1016/j.jfoodeng.2011.11.015

Schulze, B., Hubbermann, E. M., & Schwarz, K. (2014). Stability of quercetin derivatives in vacuum impregnated apple slices after drying (microwave vacuum drying, air drying, freeze drying) and storage. *LWT - Food Science and Technology, 57*(1), 426–433. https://doi.org/10.1016/j.lwt.2013.11.021

Segura-Ponce, L. A., Soto-Pardo, V. A., & Guzmán-Meza, M. F. (2019). Characterization of apples (Granny Smith) dried in industrial equipment and the relationship with drying mechanisms. *Food Structure, 21*, 100–119. https://doi.org/10.1016/j.foostr.2019.100119

Silva, W., Avendaño, N., Núñez, H., Ramírez, C., Almonacid, S., & Simpson, R. (2020). CO2 laser drilling coupled with moderate electric fields for enhancement of the mass transfer phenomenon in a tomato (Lycopersicon esculentum) peeling process. *Journal of Food Engineering, 276*, 1–10. https://doi.org/10.1016/j.jfoodeng.2019.109870

Simpson, R., Jaques, A., Núñez, H., Ramírez, C., & Almonacid, S. (2013). Fractional calculus as a mathematical tool to improve the modeling of mass transfer phenomena in food processing. *Food Engineering Review, 5*, 45–55. https://doi.org/10.1007/s12393-012-9059-7

Simpson, R., Ramírez, C., Birchmeier, V., Almonacid, S., Moreno, J., Nuñez, H., & Jaques, A. (2015). Diffusion mechanisms during the osmotic dehydration of Granny Smith apples subjected to a moderate electric field. *Journal of Food Engineering, 166*, 204–211. https://doi.org/10.1016/j.jfoodeng.2015.05.027

Simpson, R., Ramírez, C., Núñez, H., Jaques, A., & Almonacid, S. (2017). Understanding the success of Page's model and related empirical equations in fitting experimental data of diffusion phenomena in food matrices. *Trends in Food Science & Technology*, 194-201. https://doi.org/10.1016/j.tifs.2017.01.003

Simpson, R., Núñez, H., Jaques, A., Ramírez, C., Quiróz, N., Moreno, J., & Sastry, S. (2018). Application of a moderate electric field for the potential acceleration of the salting process of Atlantic salmon (Salmo salar). *Journal of Food Process Engineering*, 1-9. https://doi.org/10.1111/jfpe.12846

Singh, I. (2013). Method and apparatus for plasma assited laser cooking of food products. *US 2013/0344208 A1. 14*.

Sosa, N., Salvatori, D. M., & Schebor, C. (2012). Physico-chemical and mechanical properties of apple disks subjected to osmotic dehydration and different drying methods. *Food and Bioprocess Technology, 5*, 1790–1802. https://doi.org/10.1007/s11947-010-0468-4

Sturm, B., Nunez, V., & A. M., & Hofacker, W. C. (2014). Influence of process control strategies on drying kinetics, colour and shrinkage of air dried apples. *Applied Thermal Engineering, 62*, 455–460. https://doi.org/10.1016/j.applthermaleng.2013.09.056

Tanzi, E., Lupton, J., & Alster, T. (2003). Lasers in dermatology: Four decades of progress. *Journal of the American Academy of Dermatology, 49*, 1–31. https://doi.org/10.1067/mjd.2003.582

Tavera-Quiroz, M. J., Urriza, M., Pinotti, A., & Bertola, N. (2014). Development and characterization of a baked snack from rings of green apple. *Food and Bioprocess Technology, 7*, 2218–2227. https://doi.org/10.1007/s11947-014-1310-1

Tontul, I., Kasimoglu, Z., Asik, S., Atbakan, T., & Topuz, A. (2017). Functional properties of chickpea protein isolates dried by Refractance Window drying. *International Journal of Biological Macromolecules*. https://doi.org/10.1016/j.ijbiomac.2017.11.135

Ulloa, M. J. S. (2018). *Aplicacón de microperforaciones utilizando láser-CO2 en el proceso de liofilización de alimentos en el tiempo de secado primario*. Master's thesis. Federico Santa María Technical University., Valparaíso, Chile.

Vega-Gálvez, A., Ah-Hen, K., Chacana, M., Vergara, J., Martínez-Monzó, J., García-Segovia, P., Lemus-Mondaca, R., & Scala, K. (2012). Effect of temperature and air velocity on drying kinetics, antioxidant capacity, total phenolic content, colour, texture and microstructure of apple (var. Granny Smith) slices. *Food Chemistry, 132*, 51–59. https://doi.org/10.1016/j.foodchem.2011.10.029

Velić, D., Planinić, M., Tomas, S., & Bilić, M. (2004). Influence of airflow velocity on kinetics of convection apple drying. *Journal of Food Engineering, 64*(2004), 97–102. https://doi.org/10.1016/j.jfoodeng.2003.09.016

Velickova, E., Winkelhausen, E., & Kuzmanova, S. (2013). Physical and sensory properties of ready to eat apple chips produced by osmo-convective drying. *Journal of Food Science and Technology*. https://doi.org/10.1007/s13197-013-0950-x

Veloso, G., Simpson, R., Nuñez, H., Ramírez, C., Almonacid, S., & Jaques, A. (2021). Exploring the potential acceleration of the posmotic dehydration process via pre-treatment with CO2 laser microperforations. *Journal of Food Engineering, 306*, 110610. https://doi.org/10.1016/j.jfoodeng.2021.110610

Wairimu, G. (2011). *Study on effects of CO2 laser machining conditions on cut parameters and microstructures*. Master's thesis. Jomo Kenyatta University of Agriculture and Technology, Juja, Kenia.